Biochemical and Biophysical Research Communications **269,** 25–30 (2000)
doi:10.1006/bbrc.2000.2261, available online at http://www.idealibrary.com on IDEAL®

Digital Fluorescence Imaging of Trafficking of Endosomes Containing Low-Density Lipoprotein in Brain Astroglial Cells[1]

Tomomitsu Ichikawa,* Makoto Yamada,† Daisaku Homma,* Richard J. Cherry,‡ Ian E. G. Morrison,‡ and Suguru Kawato*,[2]

**Department of Biophysics and Life Sciences, Graduate School of Arts and Sciences, University of Tokyo at Komaba 3-8-1, Meguro, Tokyo 153, Japan; †Department of Physics, School of Medicine, Kyorin University, Mitaka, Tokyo 181, Japan; and ‡Department of Biological Sciences, University of Essex, Central Campus, Colchester CO4 3SQ, United Kingdom*

Received January 12, 2000

We have used digital fluorescence microscopy to examine transport of LDL-containing endosomes in rat brain astroglial cells to show that individual middle endosomes undergo rapid transitions between forward/backward movements and immobile states over short distances. The population of rapidly moving endosomes (>0.04 μm/sec) was 35.9%, and the remaining endosomes were slowly moving or temporarily immobile (<0.04 μm/sec). The averaged motion was, however, a very slow perinuclear motion with a velocity of 3.25 μm/h. This small velocity is mainly due to frequent changing of directions in movements, requiring 6 h for a significant concentration around the circumference of the cell nuclei. The application of both anti-dynein antibodies and vanadate in permeabilized cells resulted in peripherally concentrated distribution of endosomes, probably due to inhibition of perinuclear motion by dynein-like motor proteins. These results imply that both dynein-like and kinesin-like proteins bind to the same endosome resulting in both perinuclear and peripherally directed movements. © 2000 Academic Press

Astroglial cells guide neuronal development, metabolize ions and neurotransmitters, and regulate central nervous system vasculature (1). Neurosteroid synthesis is observed in neuroglial cells such as astrocytes and oligodendrocytes (2, 3). Neurosteroids are demonstrated to acutely modulate neurotransmitter receptors and thereby to affect neuron–neuron communications. We have recently reported the uptake of low density lipoprotein (LDL) and the existence of neurosteroidogenic proteins in astrocytes (4). Neurosteroid synthesis may occur by hydroxylation of steroids by cytochrome P450. Cholesterol is utilized in mitochondria where cytochrome P450scc cleaves a side-chain of cholesterol, resulting in pregnenolone production. Pregnenolone would be transformed into pregnenolone sulfate which modulates the NMDA subtype of glutamate receptors (5).

LDL is a carrier of cholesterol and cholesterol esters which are substrates for steroidogenesis. LDL is incorporated into endosomes via LDL receptor-mediated endocytosis (6). In rat astrocytes, LDL is endocytosed, and then delivered to lysosomes where LDL molecules are digested (7). Free cholesterol may be then transported to mitochondria. Also free cholesterol may be transferred to cholesterol ester and stored in the cytoplasm until used.

There are several reports which suggest that LDL may be supplied from blood to astrocytes. LDL was shown to be transcytosed across the blood-brain barrier (8). The trace amount of LDL was observed in cerebrospinal fluid (9). The receptor of LDL was suggested to participate in cholesterol uptake of glial cells (10). There has been little real-time analysis of LDL-containing endosome traffics in individual glial cells. We employed digital fluorescence microscope and single endosome tracking analysis to clarify molecular mechanism of intracellular endosome transport in the time scale of minutes to hours.

EXPERIMENTAL PROCEDURES

Chemicals. Dioctadecyl tetramethylindocarbocyanine perchlorate (DiI) was purchased from Molecular Probes (Eugene, OR); acridine orange, Sodium orthovanadate, and saponin were from Wako (Tokyo, Japan). Monoclonal anti-dynein mouse IgG, clone No. 70.1, was purchased from Sigma.

Abbreviations used: cytochrome P450scc, cytochrome P450 having cholesterol side-chain cleavage activity (P45011A1); DiI, dioctadecyl tetramethylindocarbocyamine perchlorate; LDL, low density lipoprotein; MEM, Dulbecco's modified Eagle's medium.

[1] This work is supported by grants from the Ministry of Education, Science and Culture in Japan and from BBSRC in the UK.

[2] To whom correspondence should be addressed. Fax: 81-3-5454-6517. E-mail: kawato@phys.c.u-tokyo.ac.jp.

0006-291X/00 $35.00
Copyright © 2000 by Academic Press
All rights of reproduction in any form reserved.

Preparation of astroglial cell cultures. Primary brain cell cultures were prepared from male Wistar rat embryo E20 as previously described. After a final centrifugation, the cell pellet was resuspended (1×10^6 cells/ml) in MEM solution containing 5% calf serum, 0.4% glucose, 0.3% $NaHCO_3$, 292 μg/ml glutamine, and 100 μg/ml kanamycin in a tissue culture dish. After 2–4 weeks of culture, when confluence had been attained, the cultured cells were trypsinized, dispersed in MEM solution, and replated at a density of 1×10^6 cells/ml. The culture medium was renewed on the third day of the culture. For microscopic observation, cells were plated onto 35-mm-diameter glass-bottom dishes previously coated with poly-L-lysine. The cells were cultured for 4–5 days at a cell density of 0.8×10^4 cells/cm^2. The purity of the cultured astrocytes were determined by immunostaining of the cells with antibody against glial fibrillary acidic protein (GFAP), showing more than 95% of cells were GFAP positive.

Isolation and labeling of LDL with DiI. LDL was isolated from fresh bovine blood by the modified method of Havel *et al.* (11). DiI was dissolved in DMSO, and 400 μl of the solution (2 mM) was incubated with 1.6–1.9 mg/ml of LDL in a total volume of 3 ml at room temperature for 2 h. Large DiI aggregates were removed by filtration of solutions with 0.20 μm of pore size. Unbound free DiI was removed from labeled LDL by microcentrifugation through a Sephadex G-25 column.

Fluorescence imaging and analysis. We used a video-enhanced fluorescence microscope equipped with a SIT camera (Hamamatsu Photonics C-1145, Japan) and with the temperature chamber which maintained the air atmosphere at 37°C. For DiI-LDL, we used 510–560 nm for excitation and fluorescence above 590 nm was selected with filters and DM580 dichroic mirror. Oil immersion objective lens of ×60 was used for single endosome tracking analysis, and dry objective lens of ×40 was used for all other experiments. The video output was digitized and the images were stored in frame memory. Data acquisition and image analysis were performed with ARGUS-50 system (Hamamatsu Photonics, Japan).

Single endosome tracking analysis. The procedures required to track fluorescent particles through time-lapse images have been given in detail elsewhere (12). The endosomes containing DiI-LDL appeared as spots covering a number of pixels with diameter of 0.5–1.0 μm; their approximate positions were identified by a simple image analysis algorithm, and then quantified by least-squares fitting the pixels in this immediate area with a 2-dimensional Gaussian function. After quantification of the spots, they were linked through the time-lapse images by a "nearest spot with similar intensity" probability method.

We assigned individual tracks of endosome movement to be directed motions with retrograde motions along the microtubules. This analysis was based on the following experimental evidences which support the middle endosome movements along microtubule networks using dynein-like and kinesin-like motor proteins: (a) Depolymerization of microtubules by the presence of nocodazole completely inhibited the endosome movement. (b) Specific inhibitors of dynein motors considerably changed the endosome movement. In this case of directed motion, the displacement R_k^i and the velocity vector $\mathbf{V}_k^i$ of the ith endosome were calculated at time $k\delta t$ using kth and $(k + 1)$th images, where the $\mathbf{r}_k^i$ is a position vector of the ith endosome in kth image and δt is the time interval between images using 1.4 sec.

$$[R_k^i]^2 = [x(k\delta t + \delta t) - x(k\delta t)]^2 + [y(k\delta t + \delta t) - y(k\delta t)]^2 \quad \text{[I]}$$

$$\mathbf{V}_k^i = (\mathbf{r}_{k+1}^i - \mathbf{r}_k^i)/\delta t \quad \text{[II]}$$

The minus end of microtubules anchors in the centrosome close to the nucleus and the plus end of microtubules is positioned around cell peripherals. Because microtubules have curved structure between these two ends, the directions of microtubules was often not parallel to the straight vector from the cell peripheral to the nucleus. For quantitative analysis of perinuclear motion of endosomes, we calculated the perinuclear velocity Vpn_k^i and peripherally directed velocity Vph_k^i using the inner products:

$$\mathrm{Vpn}_k^i = (\mathbf{V}_k^i, \mathbf{W}_i), (\mathbf{V}_k^i, \mathbf{W}_i) > = 0 \quad \text{[III]}$$

$$\mathrm{Vph}_k^i = (\mathbf{V}_k^i, \mathbf{W}_i), (\mathbf{V}_k^i, \mathbf{W}_i) < 0 \quad \text{[III']}$$

where $\mathbf{W}_i$ is a unit basis vector from the initial position of the i-th endosome to the center of cell nucleus.

RESULTS

Perinuclear Movement and Concentration of Middle Endosomes

The formation of middle endosomes with 0.5–1.0 μm in diameter appeared about 60–90 min after the 10-min of pulse LDL addition. At 60–180 min after the LDL addition, the middle endosomes were distributed almost uniformly over the entire cytoplasmic space (Fig. 1). The diameter of middle endosomes estimated from the variance of 2D-Gausian fitted fluorescent spots was distributed as follows: between 0.4–0.5 μm (11.7%), between 0.5–1.0 μm (86.5%), and between 1.0–1.5 μm (1.8%). Each middle endosome continuously showed saltatory motions containing forward/backward motions and immobile states over the time range from 1 h to 6 h after the LDL addition. The middle endosomes showed very slow perinuclear movement, resulting in a concentration of the middle endosomes around the circumference of nuclei at 6 h after the LDL addition. To quantify the degree of endosome concentration around the nucleus, we evaluated the ratio of fluorescent intensity of the doughnut-type distinct dense fluorescent region at immediately outside of the nucleus, having a band width equal to the radius of nucleus, to the total cytoplasmic fluorescent intensity in individual cells. The degree of endosome concentration was found to be 21.8 ± 6.5% at 1 h, 41.5 ± 5.1% at 3 h and 80.2 ± 7.8% at 6 h after the LDL addition. These concentrated endosomes were late endosomes having acidic pH around 5, because they showed strong fluorescence with acridine orange staining. Middle endosomes, which undergo perinuclear movement before the concentration around nuclei, were not stained with acridine orange. To identify middle endosomes and late endosomes, cells were doubly fluorescent stained with the DiI-labeled LDL and acridine orange. However, we could not distinguish between late endosomes and lysosomes both of which were acidic with pH ~5 and mainly localized around the nuclei.

Effect of Depolymerization of Microtubules by Nocodazole

To examine the possibility of endosome sliding on the microtubule networks, we depolymerized microtubules by nocodazole. After the preincubation of cells with 10

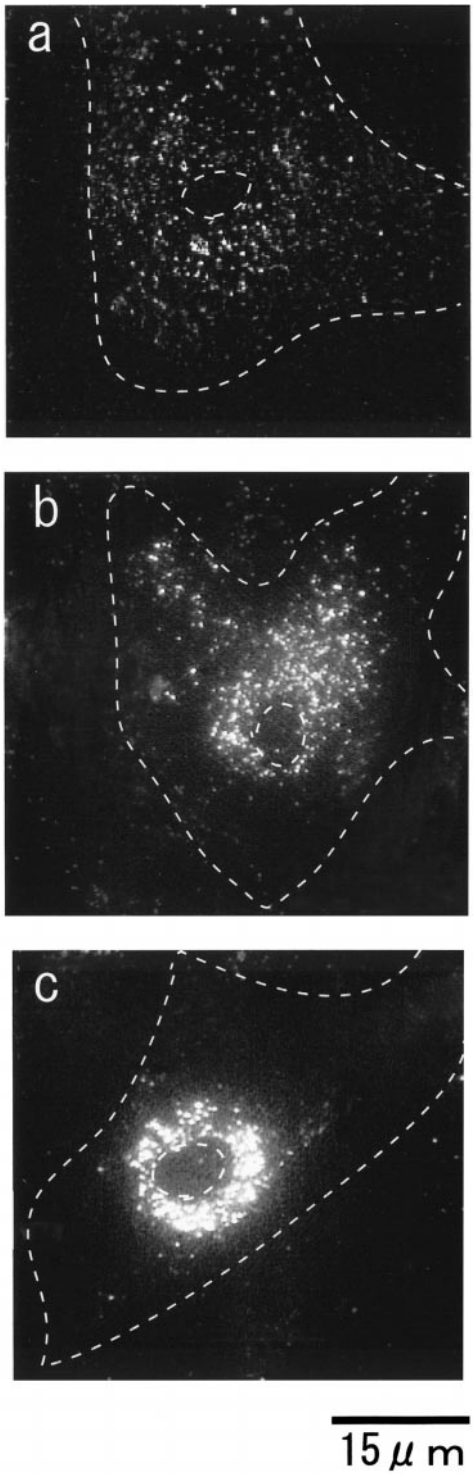

FIG. 1. Fluorescence images of the distribution of endosomes in astrocytes. Cells were incubated for 1 h (a), 3 h (b), and 6 h (c) at 37°C after the pulse addition of DiI-LDL. The circumferences of cells are indicated with white dotted lines. The scale is indicated with a horizontal black bar.

μM nocodazole for 3 h, DiI-LDL was added and endosome distribution was observed at 1, 3, 6 and 12 h later than the nocodazole treatment. Nocodazole-treated cells showed no significant concentration of endosomes around the circumference of nuclei even at 3, 6 and 12 h after the LDL addition, however, the middle endosome formation was observed at 1 h after the LDL addition. When nocodazole was removed by replacing the outer medium with the Hepes medium, a significant concentration of endosomes around the nuclei was then observed at 6 h after the nocodazole depletion. These results imply that endosomes undergo movement along microtubule networks.

We also examined the effect of actin filament disruption by applying 100 nM cytocharasin D, at 15 min before the LDL addition or at 90 min after the LDL addition. In cytocharasin D-preincubated cells, formation of middle endosomes was inhibited. When cytocharasin D was applied at 90 min after the LDL addition, we found no difference in the middle endosome formation and their concentration around nuclei in comparison with the control cells. These results suggest that actin microfilaments are involved in the formation of middle endosome but do not participate in their movements in the cytosol.

Modulation of Dynein by Anti-Dynein Antibody and Vanadate

We investigated the possible contribution of dynein-like proteins and kinesin-like proteins which may carry endosomes along microtubule networks. For inhibition of dynein-like motor proteins, cells were permeabilized with 0.05% saponin, and incubated for 15 min with anti-dynein antibody (clone 70.1) at 1:100 dilution in modified lysis buffer containing 1 mM ATP (13). The antibody was added at 90 min after the pulsed LDL addition. The presence of anti-dynein antibody prevented the concentration of endosomes around nuclei, resulting in the appearance of endosomes around the cell peripheral at 4 h after LDL addition (Fig. 2). We also applied low dose of vanadate to modulate dynein-like motor proteins. Cells were incubated with the lysis buffer containing 10, and 50 μM freshly prepared vanadate as a substitute for dynein antibody. We observed peripheral distribution of the LDL endosomes under these vanadate conditions with no significant concentration of endosomes around the circumference of nuclei. This peripherally-directed motion of endosomes was observed in less than 50 μM vanadate but the formation of middle endosomes was never inhibited. In these conditions, we checked microtubule distribution by Cy2 immunostaining. Our interpretation of these results is that inhibition of dynein-like proteins by either antibody or vanadate prevents perinuclear motion and causes facilitated anti-perinuclear motion induced by kinesin-like motor proteins. It should be noted that according to this interpretation, a middle endosome contains must contain both dynein and kinesin.

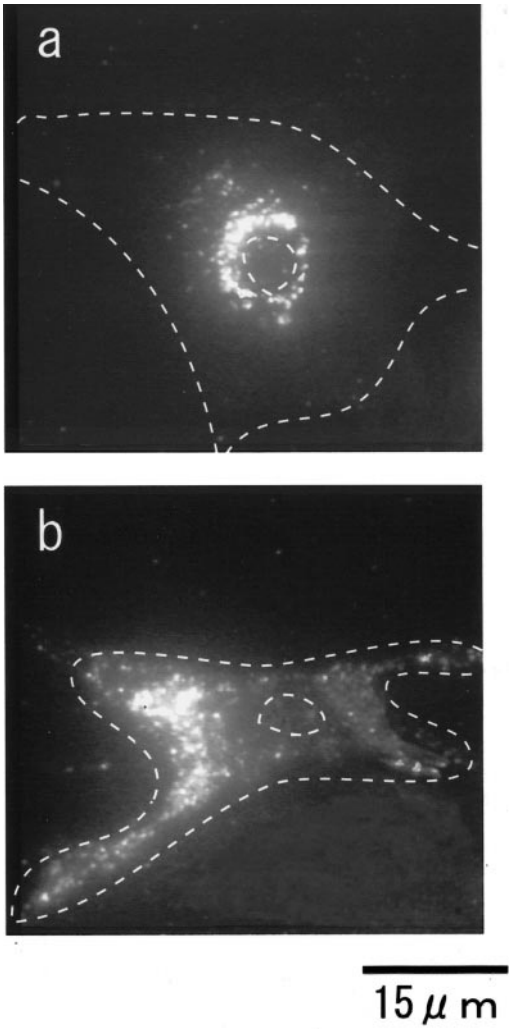

FIG. 2. Effect of antibody against dynein on the endosome movement. (a) Distribution of endosomes in control cells at 6 h after the pulse addition of LDL. Note that cells were treated by the same procedures as (b) with lysis buffer except anti-dynein IgG. (b) Distribution of endosomes in the presence of anti-dynein antibody at 4 h after the LDL addition. Anti-dynein IgG was incorporated into cells at 90 min after the LDL addition.

Directed Motion of Individual Endosomes with a Period of Retrograde Motions along the Microtubule Networks

We performed single endosome tracking analysis in order to investigate the detailed motion of individual endosomes. Figure 3 shows typical trajectories of middle endosomes in astroglial cells at 3 h after LDL addition over a time of 84 sec. Endosomes exhibited three different types of movement along the microtubules: forward motion, backward motion, and an immobile state. Many of these apparently immobile endosomes began to undergo rapid movement after a period of several minutes, implying that they were not permanently immobile. Conversely some of rapidly moving endosomes became immobile for a period of time when we traced them over several minutes. Thus endosomes appear to switch between mobile and immobile states.

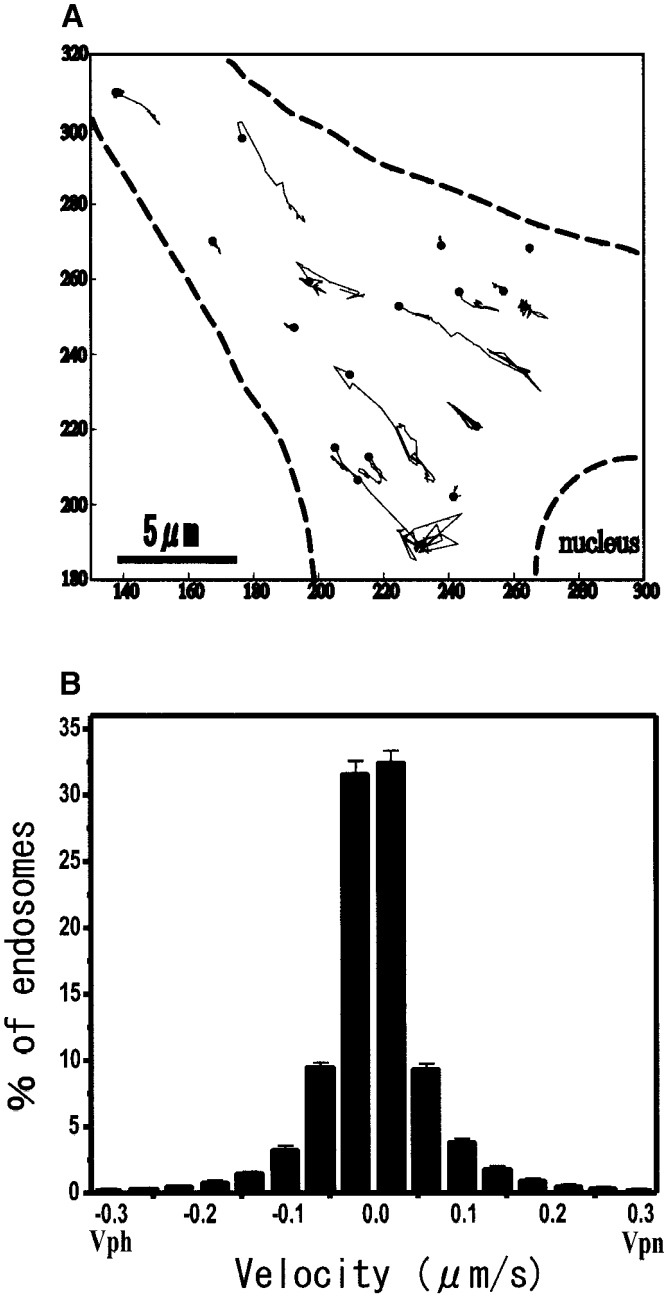

FIG. 3. Trajectories of individual endosomes in astrocytes and their velocity distribution. (A) Trajectories of middle endosomes over 84 sec from 60 successive images. These images were taken at 3 h after the pulse LDL addition. The edge of the nucleus of the cell is placed in the bottom-right corner. (B) Velocity distribution of the middle endosomes. Velocities are averaged over 84 sec for each endosomes. The positive and negative values correspond to the velocity of perinuclear motion, Vpn, and peripherally directed motion, Vph, respectively. The distribution was analyzed at 3 h after the LDL addition. Data were obtained from 32 cells in several tens of independent experiments. Error bar means SE.

A quantitative analysis of perinuclear directed motions was performed by calculating the perinuclear velocity, Vpn, and peripherally-directed velocity, Vph. Figure 3 shows histograms of the distribution of Vpn (positive horizontal axis) and Vph (negative horizontal axis) which were averaged over 84 sec for each endosomes at 3 h after the LDL addition. The quantitative analysis showed that the population of rapidly moving endosomes (>0.04 μm/sec) was 35.9% at 3 h after the LDL addition. The remaining endosomes were slowly moving or temporary immobile with a velocity slower than 0.04 μm/sec. Most of the rapidly moving endosomes were transported bidirectionally (forward and backward) with a velocity of 0.04–0.24 μm/sec (32.3%). Less than 3.6% of endosomes had a rate greater than 0.24 μm/sec at 3 h after the LDL addition. The 51% of endosomes that undergo perinuclear motion slightly exceed the endosome population of 49% having peripherally-directed motion at 3 h after the LDL addition. When many tracks of endosomes were averaged, the averaged motion showed very slow perinuclear motion with a velocity of 3.25 μm/h. Until endosomes reached the circumference of the nuclei, they move over 20 μm needing almost 6 h to go across from the cell periphery, as a sum of forward, backward and immobile movements. Once endosomes became located around the nuclei, these large endosomes became permanently immobile even in the time scale of hours. Although the real endosome movement is 3-dimensional, we performed the 2-dimensional approximation for the analysis of endosome movement because of the following considerations: Because the thickness of the cytoplasmic space was smaller than 1μm determined with confocal microscopy, the contribution of the vertical movement could be less than ~1/20 of the possible horizontal movement of ~20 μm (half diameter of the cell). Around the nuclei having the thickness of 2–3 μm, endosomes did not move considerably not only horizontally but also vertically, therefor they do not significantly contribute to the vertical movement.

DISCUSSION

We focused on the analysis of the intracellular transport of the middle endosomes. The middle endosomes carry a long distant transport of cholesterol across the cytoplasmic space, while the movements of early and late endosomes were relatively small in distance.

Dynein antibodies caused peripherally directed motion of middle endosomes due to inhibition of dynein-like motors. The selective binding of anti-dynein IgG to astrocyte dynein-like protein was demonstrated by Western immunoblotting, showing the single immunoreactive band at about 70 kDa which might be a dynein intermediate chain. Anti-dynein antibody (70.1) was reported to inhibit cytoplasmic dynein in cultured cod melanophores, resulting in the pigment movement toward the cell periphery (14). We also demonstrated that a low-dose of vanadate at 10–50 μM selectively inhibited dynein-like motors, inducing peripherally-directed motion of endosomes. In melanophores, 50 μM of vanadate selectively inhibited retrograde motion, inducing melanosomes dispersion caused by antiretrograde-directed kinesin bound to the same melanosomes (14). The requirement of higher concentrations of vanadate (10–50 μM) for dynein inhibition than those needed for inhibition of the Mg-ATPase activity of purified cytoplasmic dynein (around 1 μM) may be due to the existence of many ATP binding sites in intact cells other than dyneins (15).

The above results can be interpreted as indicating that both dynein- and kinesin-like proteins bind to same endosomes. If only dynein motors bind to endosomes, peripherally directed motion of endosomes cannot be induced by the presence of dynein antibody. If only kinesin motors bind to endosomes, generally perinuclear motion could not occur. This view of endosomes containing both dynein and kinesin motors is consistent with our observation that middle endosomes frequently changed direction of motion between forward and backward directions. Many endosomes that are immobile over a short time range of several minutes are probably detached from microtubules.

Although individual endosomes undergo rapid forward/backward movements and immobile states on a short time scale, on a long time scale these different movements of endosomes are averaged, resulting in the very slow perinuclear motion. The results lead to a novel quantitative picture of cholesterol transport in glial cells.

REFERENCES

1. Walz, W. (1995) *in* Receptors of Physiology in Neuroglia (Ketterman, H., and Ranson, B. R., Eds.), pp. 185–319. Oxford University Press, New York.
2. Baulieu, E. E., and Robel, P. (1990) *J. Steroid Biochem. Mol. Biol.* **37,** 395–403.
3. Mellon, S. H., and Deschepper, C. F. (1993) *Brain Res.* **629,** 283–292.
4. Kimoto, T., Asou, H., Ohta, Y., Mukai, H., Chernogolov, A. A., and Kawato, S. (1997) *J. Pharm. Biomed. Anal.* **15,** 1231–1240.
5. Wu, F. S., Gibbs, T. T., and Farb, D. H. (1991) *Mol. Pharmacol.* **40,** 333–336.
6. Kovanen, P. T., Faust, J. R., Brown, M. S., and Goldstein, J. L. (1979) *Endocrinology* **104,** 599–609.
7. Guillaume, D., Bertrand, P., Dea, D., Davignon, J., and Poirier, J. (1996) *J. Neurochem.* **66,** 2410–2418.
8. Dehouck, B., Fenart, L., Dehouck, M. P., Pierce, A., Torpier, G., and Cecchelli, R. (1997) *J. Cell Biol.* **138,** 877–889.

9. Salen, G., Berginer, V., Shore, V., Horak, I., Horak, E., Tint, G. S., and Shefer, S. (1987) *N. Engl. J. Med.* **316,** 1233–1238.
10. Jung-Testas, I., Weintraub, H., Dupuis, D., Eychenne, B., Baulieu, E. E., and Robel, P. (1992) *J. Steroid. Biochem. Mol. Biol.* **42,** 597–605.
11. Havel, R. J., Eder, H. A., and Bragdon, J. H. (1955) *J. Clin. Invest.* **34,** 1345–1353.
12. Wilson, K. M., Morrison, I. E., Smith, P. R., Fernandez, N., and Cherry, R. J. (1996) *J. Cell. Sci.* **109,** 2101–2109.
13. Grundstrom. N., Karlsson, J. O., and Andersson, R. G. (1985) *Acta Physiol. Scand.* **125,** 415–421.
14. Nilsson, H., and Wallin, M. (1997) *Cell. Motil. Cytoskeleton* **38,** 397–409.
15. Hisanaga, S., and Sakai, H. (1983) *J. Biochem.* **93,** 87–98.